Title: Attenuated evolution of mammals through the Cenozoic

Authors: Anjali Goswami[1,2*], Eve Noirault[1], Ellen J. Coombs[1,2,3], Julien Clavel[4], Anne-Claire Fabre [1,5,6], Thomas J.D. Halliday[1,7], Morgan Churchill[8], Abigail Curtis[9], Akinobu Watanabe[1,10,11], Nancy B. Simmons[12], Brian L. Beatty[10,13], Jonathan H. Geisler[10,13], David L. Fox[14], Ryan N. Felice[1,2,15]

Affiliations:

[1]Department of Life Sciences, Natural History Museum; London, United Kingdom

[2]Department of Genetics, Evolution, and Environment, University College London; London, United Kingdom

[3]Department of Vertebrate Zoology, National Museum of Natural History, Smithsonian Institution; Washington, DC, United States

[4]Université Lyon, Université Claude Bernard Lyon 1, CNRS, ENTPE, UMR 5023 LEHNA, F-69622, Villeurbanne, France

[5]Naturhistorisches Museum Bern; Bern, Switzerland

[6]Institute of Ecology and Evolution, University of Bern; Bern, Switzerland

[7]School of Geography, Earth and Environmental Sciences, University of Birmingham; Birmingham, United Kingdom

[8]Department of Biology, University of Wisconsin Oshkosh; Oshkosh, WI, USA

[9]Department of Biology, University of Washington; Seattle, WA, USA

[10]Department of Anatomy, College of Osteopathic Medicine, New York Institute of Technology; Old Westbury, NY, USA

[11]Division of Paleontology, American Museum of Natural History; New York, NY, USA

[12]Department of Mammalogy, Division of Vertebrate Zoology, American Museum of Natural History; New York, NY, USA

[13] Department of Paleobiology, National Museum of Natural History, Smithsonian Institution; Washington, DC, United States

[14]Department of Earth and Environmental Sciences, University of Minnesota; Minneapolis, MN, USA

[15]Centre for Integrative Anatomy, Department of Cell and Developmental Biology, University College London; London, United Kingdom

*Corresponding author. Email: a.goswami@nhm.ac.uk

Abstract: The Cenozoic diversification of placental mammals is the archetypal adaptive radiation. Yet, discrepancies between molecular divergence estimates and the fossil record fuel ongoing debate around the timing, tempo, and drivers of this radiation. Analysis of a high-dimensional 3D skull dataset for living and extinct placental mammals demonstrates that evolutionary rates peak early and attenuate quickly. This long-term decline in tempo is punctuated by bursts of innovation that decrease in amplitude over the past 66 million years. Social, precocial, aquatic, and herbivorous species evolve fastest, especially whales, elephants, sirenians, and extinct ungulates. Slow rates in rodents and bats indicate dissociation of taxonomic and morphological diversification. Frustratingly, highly similar ancestral shape estimates for placental mammal superorders suggest that their earliest representatives may continue to elude unequivocal identification.

One-Sentence Summary: Short bursts of innovation punctuate long-term decline in the rate of placental mammal skull evolution through the "Age of Mammals".

Introduction

Placental mammals make up 94% of extant mammalian diversity, with over 6100 recognized extant species (*1*). This richness in species numbers is paired with an immense variation in ecology and morphology, with fully volant to fully aquatic forms spanning six orders of magnitude in size. Much diversification of placental mammals is thought to have been achieved quickly in the early Cenozoic, in the aftermath of the Cretaceous-Paleogene (K/Pg) mass extinction that removed non-avian dinosaurs from global ecosystems (*2*). However, despite a wealth of data from extant and fossil species, the timing, tempo, and drivers of the placental mammal morphological radiation have remained contentious. Studies of body size evolution variably support an early burst (*3*), accelerating rates linked to climate (*4*), or stable rates following the initial superordinal divergences. These studies often suggest that the K/Pg event had little impact on placental mammal evolution (*5*). In contrast, studies of tooth morphology or discrete character data suggest either that morphological diversification post-dated the K/Pg extinction (*6*, *7*) or that rates of evolution increased rapidly at K/Pg boundary (*8*). Some of this uncertainty is due to ongoing debate on the timing of origin of Placentalia and its proximity to the K/Pg mass extinction (*9–16*). Two additional critical factors contribute to this uncertainty, 1) the exclusion of fossils from most studies, despite wholly extinct lineages dominating the initial post-K/Pg fauna (*10*), and 2) the limited phenotypic data used in most analyses of the morphological diversification of placentals. Phenotype is the object of natural selection, as the interface between organisms and their environment, but most studies reduce complex morphologies to highly simplified metrics, such as body size (*11*, *12*) or discrete binary

characters (*9*, *13*), hindering robust understanding of the influence of social, ecological, and developmental factors on morphological evolution.

Here we reconstruct the pattern and drivers of the morphological diversification of Placentalia with the first quantitative analysis of cranial evolution that samples the full breadth of living and extinct placental mammal diversity. Our dense 3D morphometric dataset (757 landmarks and sliding semi-landmarks) for 322 species spans the Cenozoic Era and represents every extant family and a majority of extinct orders (Fig. 1-2, fig. S1, table S1, data S1). We focus on the cranium because it is a feature-rich structure that performs several critical functions implicated in placental mammal success, from feeding, fighting, and communication to housing and protecting sensory structures and the brain. Given the ongoing debate on the timing of placental mammal diversification and the phylogenetic positions of some extinct clades, we perform these analyses across 1800 evolutionary trees, using multiple topologies and divergence estimates spanning from 100 to 70 million years ago, thereby incorporating the impact of this chronological and phylogenetic uncertainty on our understanding of placental mammal evolution. We summarized our results by binning these phylogenetic frameworks into a total of 18 sets, divided by tree topology and 5-million-year intervals for the placental mammal root age; for example, 100 trees use tree topology 2 and a divergence estimate for Placentalia ranging between 80-85 million years ago. With these analyses, we reconstructed the tempo and mode of evolution of the placental mammal skull to robustly test the hypothesis that placental mammals radiated quickly in the aftermath of the K/Pg mass extinction and to assess the primary social, developmental, and ecological factors associated with their morphological diversification.

Results

Cranial variation across placental mammals

Despite the vast ecological range of placental mammals, skull variation is overwhelmingly concentrated into a single region of morphospace, suggesting extensive conservation or convergence of cranial form across all placental mammal superorders (Fig. 1, fig. S2). There are two other clusters observed, but each is populated by single clades, specifically whales and rodents. PC1 (34.1% of the total variation) is dominated by shifts associated with the land-to-water transition of whales, with two distinct concentrations representing "terrestrial" and "aquatic" adaptive peaks. Extreme elongation of the premaxilla and maxilla and retraction of the nasals in Cetacea drives change along this axis, with early whales overlapping substantially with terrestrial Laurasian "ungulates" including Litopterna, Perissodactyla, and Artiodactyla. Several other lineages converge on aspects of this morphology, particularly the retraction of the nasals, including Sirenia, Desmostylia, Proboscidea, and Embrithopoda. The opposite extreme of PC1 is dominated by short-faced, globular euarchontaglirans, particularly Rodentia and Primates. Whales span the full breadth of PC2 (14.9% of the total variation), with the unusual extinct walrus-like whale *Odobenocetops* defining the maximum end of the axis, and the early archaeocete *Pakicetus* at the opposite extreme. Many placental mammal lineages are better discriminated along this axis, with extremely dolicocephalic armadillos occupying lower PC2 values, and brachycephalic primates, bats, and elephants at the positive end. Rodents are further distinguished on PC3, where they form a distinct concentration of variation separate from other terrestrial placental mammals (Fig. 1, fig. S2), driven largely by the height of facial region, size of the nasals, and orientation of the occipital region. Extant and extinct taxa largely overlap in cranial morphospace, with Paleogene to Recent taxa occupying similar positions on the principal axes. Fossil forms fill the gap between the terrestrial and aquatic clusters on PC1, but they also define the extremes of most principal axes, demonstrating the exceptional extinct diversity of

placentals. In contrast, the pale fox (*Vulpes pallida*) is closest to the average cranial shape of extant placental mammals, with an extinct confamilial, the borophagine dog *Desmocyon matthewsi* possessing a skull most similar to the average shape among the sampled living and extinct mammals.

Tempo of cranial evolution across placental mammals

Bayesian analysis using a reversible-jump Markov chain Monte Carlo algorithm supported variable-rates Brownian motion with a lambda tree transformation ($\lambda = 0.629$-0.741) as the best supported model of evolution across every phylogenetic topology and divergence time bin sampled in this study (fig. S3). Despite vast differences in the estimated root age for placentals, ranging from 100 to 70 million years in the phylogenetic hypotheses included here, results are remarkably consistent, with little to no difference in positions of rate shifts or relative rates of evolution across the placental mammal tree (Fig. 2; fig. S4). Rate shifts are clustered at the base of Placentalia, varying slightly in whether they occur at the basal nodes for each superorder or more inclusive nodes (e.g. Boreoeutheria and Atlantogenata) and demonstrating an increase in rate from stem to crown Placentalia (fig. S4). High rates are also concentrated at the base of many orders, reflecting the rapid accumulation of ecological and morphological diversity early in the placental mammal radiation. Multiple rate increases occur along the stem of Cetacea, with particularly fast rates of evolution on the branches leading to fully aquatic whales (basilosaurid archaeocetes + crown cetaceans), as well as to odontocetes. High rates of evolution are also observed at or near the base of Paenungulata (and/or Sirenia, depending on phylogenetic tree), Cingulata, Primates (and/or Catarrhini), Rodentia, and Chiroptera. There are relatively fewer high rates of evolution observed in less-inclusive clades, but high rates are observed on the

branches leading to hominids, sabre-toothed cats, pinnipeds, beavers, camels, yangochiropteran bats, and the extinct large-bodied brontothere perissodactyls (Fig. 2, fig. S4).

Placing evolutionary rates in temporal context necessarily depends heavily on the divergence estimates of the phylogenetic framework. Nonetheless, the distribution of evolutionary rates across a range of phylogenetic hypotheses is strongly indicative that the tempo of cranial evolution increased rapidly early in placental mammal evolution, proximal to the end-Cretaceous mass extinction, and fell equally rapidly, in contrast to studies of body size evolution in extant taxa (*4*, *5*). This initial burst is followed by long term decline, but this decline is punctuated by multiple smaller peaks throughout the Cenozoic, a pattern that we describe as "attenuated evolution", indicating decreasing amplitude of peaks in evolutionary rate along a backdrop of declining rates. The initial radiation and declining rates are consistent with an early burst model (*18*), but the presence of numerous intermediate peaks in evolutionary rates distinguishes this pattern from a standard early burst. The declining size of those peaks likely reflects increasingly limited niche space with distance from the K/Pg mass extinction, while their timing, allowing for the aforementioned uncertainties, likely reflects subsequent bursts of diversification associated with major climatic and geologic events. Several scenarios reconstruct a large peak in rates in the early to middle Eocene and smaller peaks near the Eocene-Oligocene and Oligocene-Miocene boundaries, all of which are associated with transitions between warmer and cooler climates (Fig. 3). In contrast, the impact of the rapid warming event at the Paleocene-Eocene boundary (PETM) on evolutionary rates is ambiguous, with sharp declines, small increases, or little change in rate during this interval, depending on the estimated root age of Placentalia.

Both the slowest and the fastest evolving clades in this study are wholly extinct lineages that straddle the end-Cretaceous mass extinction (Fig. 3, fig. S5). Stem placental mammals with

unambiguous Late Cretaceous origins and a rich fossil record evolved much more slowly than all crown placental mammals in every phylogenetic framework. "Archaic" and South American native ungulates, both of which first appear in the fossil record in the Paleocene in the aftermath of the mass extinction, display the fastest rates of evolution in every scenario. Comparing overall rates of cranial evolution across orders also demonstrates a clear dissociation of taxonomic diversification and morphological evolution in the crown placental mammal radiation. Irrespective of topology and divergence estimates, laurasiatherian and afrotherian clades display the fastest rates of cranial evolution (Fig. 3; fig. S5), while the most speciose placental mammal orders, Rodentia and Chiroptera, show some of the lowest evolutionary rates for cranial shape. The relative ranking among the five orders with the fastest rates of cranial evolution varies depending on topology and divergence time bin, but always includes: Cetacea, Proboscidea, Sirenia, and the extinct orders Litopterna and "Amblypoda" (a likely paraphyletic grouping of early Cenozoic large-bodied ungulates). Interestingly, members of the defunct, paraphyletic "Insectivora", including Afrosoricida, Macroscelidea, Scandentia, and Eulipotyphla, consistently show some of the slowest rates of evolution, which may have contributed to the long-standing difficulties with ascertaining their phylogenetic relationships based on morphology alone.

Among extant superorders, Euarchontoglires is consistently the slowest evolving, with all clades, including rodents and primates, exhibiting some of the slowest evolutionary rates among placentals. The xenarthran clades all consistently display an intermediate rate of evolution relative to other placentals, while laurasiatherians show the broadest range of evolutionary rates across orders. Other than the fast-evolving aquatic or extinct ungulates and slow-evolving bats noted above, the other laurasiatherians show a division between herbivorous ungulate orders (Artiodactyla, Perissodactyla, and Notoungulata) that evolve at moderate rates, while

carnivorous laurasiatherians, including Carnivora and the extinct creodonts, display relatively slow rates of evolution. While we do not quantify taxonomic diversification in this study, our results do suggest that the expected close association of rates of speciation and rates of phenotypic evolution may not extend cleanly to the placental mammal skull. This expectation stems from theories of positive coupling between lineage splitting and adaptation to new niches via phenotypic evolution (*19*). In contrast, numerous examples exist of taxonomic diversification occuring in the absence of ecological or morphological divergence (*20*). Recent study of rates of body size evolution and speciation in several vertebrate clades identified a general relationship between these two rates within each vertebrate class, but noted that the strength of this association varied widely in subclades within each class. Moreover, some smaller clades displayed a negative relationship between rate of speciation and that of body size evolution (*20*). Similarly, the lack of a clear association between taxonomic diversity and rate of cranial evolution across placental mammals does not preclude a stronger association existing within placental mammal clades. A focused analysis of this relationship, taking into account ongoing debate on the ability to accurately estimate rates of taxonomic diversification (*21*), is needed, but it is worth considering whether the likely drivers of non-adaptive radiations, such as geographic isolation, may be more pronounced in smaller taxa, such as those that dominate the two most speciose placental mammal clades, Rodentia and Chiroptera.

Drivers of cranial evolution in placental mammals

We further examined the influences of size, diet, and locomotion on skull shape and rate of cranial evolution using multivariate phylogenetic linear models fitted by penalized likelihood, across the same distribution of phylogenetic tree topologies and divergence time bins described above. The additional factors of habitat, development (altricial/precocial), diel activity pattern,

and social structure (social/solitary) were further examined for the 207 extant species (data S1). When limited to extant taxa, size and diet were the only factors consistently supported as significantly influencing cranial shape and significantly interacting with each other across all phylogenetic frameworks and time bins ($p < 0.05$; table S2). Locomotion has a significant, albeit lower, effect on skull shape in all but the youngest divergence time bin (70-75Ma), whereas habitat type was supported as a significant factor in a minority of analyses. Analyses including extinct taxa are congruent with these results, including diet and size showing the strongest and most consistent influence on cranial shape, as well as having a significant interaction (table S2). Shape changes associated with increased size are concentrated in the elongation of the rostral region (fig. S6), as suggested by previous studies (*22*). Large size is additionally associated with retraction of the nasals, noted in numerous lineages as described above. Variation associated with dietary categories also reflects traits long identified as informative for ecomorphological analyses, including a larger sagittal crest in carnivores, reduced zygomatics in social insectivores, and rostrum elongation and cranial telescoping in bulk invertivores (a category composed entirely of cetaceans).

Although most of the factors we examined are not significantly associated with cranial shape, there are substantial differences in the rate of cranial evolution associated with these factors, which could be informative for modelling species response to environmental change. In particular, diet, locomotion, social structure, and development show significant differences in cranial rate among character states (Fig. 4, fig. S7). Dietary categories dominated by aquatic taxa, specifically bulk invertivores and piscivores, evolve the fastest, followed by herbivores. Aquatic and semi-aquatic mammals evolve fastest among locomotor categories, with arboreal and semi-arboreal showing comparatively slow evolution. Aquatic mammals similarly

dominated among habitat categories, whereas desert taxa exhibit a broad range of rates. Notably, social animals evolve significantly faster than solitary animals, potentially due to pressure for elaborate cranial ornamentation in many social species. Precocial species also evolve at a strikingly faster rate than altricial mammals, suggesting that extended parental care of young may result in overall slower rates of evolution. Placental mammals without a fixed period of activity, a category dominated by fast-evolving whales and proboscideans, evolve more rapidly than diurnal, nocturnal, or crepuscular species, but there are surprisingly no significant differences among taxa displaying these latter three activity patterns. Some of these patterns, such as fast rates in bulk invertivores, are clearly driven by cetaceans. However, several of the character states exhibited by some or most cetaceans are shared with other placentals, and these non-cetacean taxa also display higher rates of evolution. For example, aquatic mammals in this dataset include cetaceans, pinnipeds, sirenians, and desmostylians, all of which display elevated rates of skull evolution. Other character states associated with higher rates of evolution, such as precociality, sociality, and cathemeral activity pattern, are observed across placentals. In particular, these states are exhibited by many terrestrial herbivores (another fast-evolving ecological group), as well as cetaceans (fig. S8), demonstrating that these results are not solely driven by a single, fast-evolving clade.

Although not considered explicitly here, we may expect postcranial systems to diverge from the patterns observed here, particularly in terms of the differences across clades. Specifically, we may expect higher rates of postcranial evolution in bats and euarchontans, as well as in arboreal and semi-arboreal taxa more generally, in contrast to the low rates of cranial evolution observed for these groups here. More similarity in temporal pattern of cranial and postcranial evolution is likely, as those are likely driven by extrinsic phenomenon, such as mass extinctions or large-

scale environmental change. However, some of the most extreme postcranial transitions, associated with the appearance of fully aquatic or fully volant mammals, occur during the Eocene. Quantifying postcranial evolution would thus likely increase the amplitude of evolutionary rates during that interval, but further work along these lines is needed to test this hypothesis.

Ancestral estimations of the earliest placental mammals and implications for resolving their origins

Finally, we used our extensive sample of living and extinct placental mammals to estimate cranial shapes for the most recent common ancestor (MRCA) of placental mammals and of each of the four placental mammal superorders (Fig. 3). Regardless of the starting 3-D mesh used (shown here for *Vulpes pallida*, the most average extant placental mammal in this sample), ancestral estimates for the four superorders are remarkably similar, with only the euarchontogliran MRCA distinguished by a broader vault and a shorter and narrower rostrum. Subtle differences among all superordinal MRCAs exist, largely in the breadth and tapering of the rostrum. However, the similarities in these ancestral reconstructions may explain the persistent difficulties with identifying unambiguous Cretaceous crown placentals, despite the near certain divergence of the superorders in advance of the end-Cretaceous mass extinction. Rather than reflecting shortcomings of the fossil record or phylogenetic methodologies, this uncertainty may be due to the lack of clear morphological differences among the earliest representatives of the placental mammal superorders (*7*). This more pernicious source of uncertainty may be unresolvable, but, fortunately, our results demonstrate that reconstructions of the tempo and drivers of the exceptional morphological diversification of placental mammals are

robust to considerable uncertainty in both phylogenetic topology and the timing of their initial radiation.

Materials and Methods

Our dataset samples 322 crown and stem placental mammals, including 207 extant and 115 extinct species. 66 3D landmarks and 69 semi-landmark curves were collected for the left side of the skull using Stratovan Checkpoint (Stratovan, Davis, CA, USA). Landmarks and semi-landmarks were imported into R for analysis, where curves were resampled to a common number of semi-landmarks, slid to minimize bending energy, and registered with Generalised Procrustes Analysis, resulting in a total of 757 3D landmarks and sliding semi-landmarks. Data on diet, locomotion, habitat, development, social structure, and activity pattern were collected from the published literature.

In the absence of a well-resolved phylogenetic hypothesis that samples all living and extinct taxa in our dataset, we constructed an extensive range of alternative phylogenies. Starting with a set of node-dated trees from the posterior distribution of a recent species-level molecular analysis of placental mammal relationships (*14*), we binned these trees into six 5-million-year bins (70-75Ma, 75-80Ma, 80-85Ma, 85-90Ma, 90-95Ma, and 95-100Ma). We then grafted in fossil taxa based on a suite of recent morphological phylogenetic analyses (see Supplementary Materials), focusing on three alternative topologies that capture the major points of uncertainty, and generating 419,400 alternative trees to capture uncertainty in divergence estimates. Finally, we subsampled this set to 1800 trees, 100 for each of the six 5-million-year root-age bins for each of the three topologies, which was used in subsequent analyses.

Macroevolutionary analyses

To examine the overall pattern of cranial variation across placentals, we conducted a principal components analysis using Procrustes-aligned 3D data and reconstructed wireframe models for the minimum and maximum shapes on the primary axes of variation. We further estimated the ancestral shape for the placental MRCA and each superordinal MRCA by maximum likelihood and warping of a reference shape to the ancestral estimates.

We assessed 10 alternative evolutionary models (variable- and single-rate models for Brownian motion, Ornstein-Uhlenbeck, and BM with lambda, kappa, or delta tree transformations) for cranial evolution using phylogenetic PC scores representing 95% of the total variation in the dataset and a reversible-jump Markov Chain Monte Carlo (MCMC) algorithm implemented in BayesTraits v. 3 (*5*). For the best supported model, we binned rates by geological time and plotted their pattern through time for one randomly selected tree from 18 alternative tree topologies and divergence estimate bins. We further extracted rates for the terminal branches and plotted them by clade to assess differences in mean rate across clades.

We assessed the association of life history and ecological traits on cranial variation and evolutionary rates using Type II phylogenetic MANOVAs (phylogenetic regressions) on the Procrustes coordinates with log centroid size and each of the six factors as predictors across the same 18 trees. We conducted one analysis of size, diet, and locomotion for the full dataset of living and extinct species (n = 322) and a second one of all six factors for just the extant taxa (n = 207). Finally, we used a state-specific Brownian motion (BMM) model to estimate rates of evolution for each ecological and life history state across the full suite of 1800 trees. Further details of all materials and methods are provided in Supplementary Materials.

References and Notes:

1. C. J. Burgin, J. P. Colella, P. L. Kahn, N. S. Upham, How many species of mammals are there? *J. Mammal.* **99**, 1–14 (2018).

2. G. G. Simpson, The beginning of the age of mammals. *Biol. Rev.* **12**, 1–46 (1937).

3. N. Cooper, A. Purvis, Body size evolution in mammals: Complexity in tempo and mode. *Am. Nat.* **175**, 727–738 (2010).

4. J. Clavel, H. Morlon, Accelerated body size evolution during cold climatic periods in the Cenozoic. *Proc. Natl. Acad. Sci. U.S.A.* **114**, 4183–4188 (2017).

5. C. Venditti, A. Meade, M. Pagel, Multiple routes to mammalian diversity. *Nature*. **479**, 393–396 (2011).

6. D. M. Grossnickle, E. Newham, Therian mammals experience an ecomorphological radiation during the Late Cretaceous and selective extinction at the K–Pg boundary. *Proc. R. Soc. B.* **283**, 20160256 (2016).

7. N. Brocklehurst, E. Panciroli, G. L. Benevento, R. B. J. Benson, Mammaliaform extinctions as a driver of the morphological radiation of Cenozoic mammals. *Curr. Biol.* **31**, 2955-2963.e4 (2021).

8. T. J. D. Halliday, P. Upchurch, A. Goswami, Eutherians experienced elevated evolutionary rates in the immediate aftermath of the Cretaceous–Palaeogene mass extinction. *Proc. R. Soc. B.* **283**, 20153026 (2016).

9. R. M. D. Beck, M. S. Y. Lee, Ancient dates or accelerated rates? Morphological clocks and the antiquity of placental mammals. *Proc. R. Soc. B.*. **281**, 20141278 (2014).

10. M. S. Springer, C. A. Emerling, R. W. Meredith, J. E. Janečka, E. Eizirik, W. J. Murphy, Waking the undead: Implications of a soft explosive model for the timing of placental mammal diversification. *Mol. Phylo.Evol.* **106**, 86–102 (2017).

11. R. W. Meredith *et al.*, Impacts of the Cretaceous terrestrial revolution and K/Pg extinction on mammal diversification. *Science*. **334**, 521–524 (2011).

12. S. Álvarez-Carretero *et al.*, A species-level timeline of mammal evolution integrating phylogenomic data. *Nature*. **602**, 263–267 (2022).

13. M. A. O'Leary *et al.*, The placental mammal ancestor and the post–K-Pg radiation of placentals. *Science*. **339**, 662–667 (2013).

14. T. J. D. Halliday, M. dos Reis, A. U. Tamuri, H. Ferguson-Gow, Z. Yang, A. Goswami, Rapid morphological evolution in placental mammals post-dates the origin of the crown group. *Proc. R. Soc. B.* **286**, 20182418 (2019).

15. N. S. Upham, J. A. Esselstyn, W. Jetz, Inferring the mammal tree: Species-level sets of phylogenies for questions in ecology, evolution, and conservation. *PLOS Biol.* **17**, e3000494 (2019).

16. N. M. Foley, M. S. Springer, E. C. Teeling, Mammal madness: is the mammal tree of life not yet resolved? *Phil. Trans. R. Soc. B.* **371**, 20150140 (2016).

17. T. R. Lyson *et al.*, Exceptional continental record of biotic recovery after the Cretaceous–Paleogene mass extinction. *Science*. **366**, 977–983 (2019).

18. L. J. Harmon *et al.*, Early bursts of body size and shape evolution are rare in comparative data. *Evol*. **64**, 2385–2396 (2010).

19. G. G. Simpson, *The Major Features of Evolution.* (Columbia University Press, New York, 1953).

20. C. R. Cooney, G. H. Thomas, Heterogeneous relationships between rates of speciation and body size evolution across vertebrate clades. *Nat. Ecol. Evol.* **5**, 101–110 (2021).

21. S. Louca, M. W. Pennell, Extant timetrees are consistent with a myriad of diversification histories. *Nature*. **580**, 502–505 (2020).

22. A. Cardini, P. D. Polly, Larger mammals have longer faces because of size-related constraints on skull form. *Nat. Commun.* **4**, 2458 (2013).

23. T. J. D. Halliday, P. Upchurch, A. Goswami, Resolving the relationships of Paleocene placental mammals. *Biol. Rev.* **92**, 521–550 (2017).

24. C. Bardua, R. N. Felice, A. Watanabe, A.-C. Fabre, A. Goswami, A practical guide to sliding and surface semilandmarks in morphometric analyses. *Integ. Org.Biol.* **1** (2019), doi:10.1093/iob/obz016.

25. S. Schlager, in *Statistical Shape and Deformation Analysis*, G. Zheng, S. Li, G. Székely, Eds. (Academic Press, 2017), pp. 217–256.

26. E. K. Baken, M. L. Collyer, A. Kaliontzopoulou, D. C. Adams, geomorph v4.0 and gmShiny: Enhanced analytics and a new graphical interface for a comprehensive morphometric experience. *Meth. Ecol. Evol.* **12**, 2355–2363.

27. J. M. Ryan, G. K. Creighton, L. H. Emmons, Activity patterns of two species of *Nesomys* (Muridae: Nesomyinae) in a Madagascar rain forest. *J. Trop. Ecol.* **9**, 101–107 (1993).

28. A. Orr, thesis, California State University Fresno (1998).

29. R. M. Nowak, E. P. Walker, *Walker's Mammals of the World* (Johns Hopkins University Press, Baltimore, 5th ed., 1991).

30. B. J. MacFadden, Cenozoic mammalian herbivores from the Americas: reconstructing ancient diets and terrestrial communities. *Annu. Rev. Ecol. Syst.* **31**, 33–59 (2000).

31. J. Kennis, C. Laurent, N. D. Amundala, A. M. Dudu, H. Leirs, Survival and movement of the Congo forest mouse (Deomys ferrugineus): a comparison of primary rainforest and fallow land in Kisangani, Democratic Republic of Congo. *Afric.Zool.* **47**, 147-159 (2012).

32. M. Kamoun, P. Steinmetz, Feeding behaviour, intake and digestion of the *Camelus dromedarious* at pasture. *Opt. Méditerr. B.* **13**, 51–57 (1995).

33. C. N. Jacques, J. D. Sievers, C. L. Sexton, D. E. Roddy, Evaluating diet composition of pronghorn in Wind Cave National Park, South Dakota, *Prairie Nat.* **12**, 239-250 (2006).

34. IUCN, The IUCN Red List of Threatened Species. Version 2021-3 (2021).

35. G. Guo, E. Zhang, Diet of the Chinese water deer (*Hydropotes inermis*) in Zhoushan Archipelago, China. *Acta Therio. Sin.*.**25**, 122–130 (2005).

36. S. Giri, A. Aryal, R. K. Koirala, B. Adhikari, D. Raubenheimer, Feeding ecology and distribution of Himalayan serow (*Capricornis thar*) in Annapurna Conservation Area, Nepal. *World J. Zool.* **6**, 80-85 (2011).

37. C. Gebert, H. Verheyden-Tixier, Variations of diet composition of Red Deer (Cervus elaphus L.) in Europe. *Mamm. Rev.* **13**, 189-201 (2001).

38. W. W. Dalquest, thesis, Louisiana State University (1953).

39. L. Costeur, O. Maridet, S. Peigné, E. P. J. Heizmann, Palaeoecology and palaeoenvironment of the Aquitanian locality Ulm-Westtangente (MN2, Lower Freshwater Molasse, Germany). *Swiss J. Palaeontol*. **131**, 183–199 (2012).

40. J. F. Connor, The mammals of the Tug Hill Plataeu, New York. *NY State Mus. Sci. Ser. Bull.* **406**, 1–82 (1966).

41. A. M. Candela, L. L. Rasia, M. E. Pérez, in *Early Miocene Paleobiology in Patagonia*, S. F. Vizcaíno, R. F. Kay, M. S. Bargo, Eds. (Cambridge University Press, ed. 1, 2012), pp. 287–305.

42. D. E. Wilson, S. Ruff, Eds., *The Smithsonian Book of North American Mammals* (Smithsonian Institution Press, Washington, 1999).

43. J. R. Schuette, D. M. Leslie, R. L. Lochmiller, J. A. Jenks, Diets of hartebeest and roan antelope in Burkina Faso: Support of the long-faced hypothesis. *Journal of Mammalogy*. **79**, 426–436 (1998).

44. J. D. Schmerge, thesis, University of Kansas (2015).

45. F. Reid, *A Field Guide to the Mammals of Central America & Southeast Mexico* (Oxford University Press, New York, 1997).

46. R. A. Pellew, The feeding ecology of a selective browser, the giraffe *(Giraffa camelopardalis tippelskirchi)*. *J. Zool.* **202**, 57–81 (1984).

47. M. C. Mihlbachler, N. Solounias, Coevolution of tooth crown height and diet in oreodonts (Merycoidodontidae, Artiodactyla) examined with phylogenetically independent contrasts. *J. Mammal Evol.* **13**, 11–36 (2006).

48. B. Kassa, R. Libois, B. Sinsin, Diet and food preference of the waterbuck (*Kobus ellipsiprymnus defassa*) in the Pendjari National Park, Benin. *Afr. J. Ecol.* **46**, 303–310 (2008).

49. C. Janis, The species richness of Miocene browsers, and implications for habitat type and primary productivity in the North American grassland biome. *Palaeogeog. Palaeoclim. Palaeoecol.* **207**, 371–398 (2004).

50. T. Hofmann, H. Roth, Feeding preferences of duiker (*Cephalophus maxwelli*, *C. rufilatus*, and *C. niger*) in Ivory Coast and Ghana. *Mamm. Biol.* **68**, 65–77 (2003).

51. A. Forsyth, *Mammals of the Canadian Wild* (Firefly Books, Scarborough, Ont., Canada, 1985).

52. S. K. Eltringham, *The Hippos: Natural History and Conservation* (Academic Press, London, 1999).

53. J. J. M. Calede, J. X. Samuels, M. Chen, Locomotory adaptations in entoptychine gophers (Rodentia: Geomyidae) and the mosaic evolution of fossoriality. *J. Morph.* **280**, 879–907 (2019).

54. I. C. R. Barbosa *et al.*, Analysing the isotopic life history of the alpine ungulates *Capra ibex* and *Rupicapra rupicapra rupicapra* through their horns. *Rapid Commun. Mass Spectrom.* **23**, 2347–2356 (2009).

55. C. Blondel, H. Bocherens, A. Mariotti, Stable carbon and oxygen isotope ratios in ungulate teeth from French Eocene and Oligocene localities. *Bull. de la Soc. Géol. de France*. **168**, 775–781 (1997).

56. D. E. Wilson, R. A. Mittermeier, Eds., *Handbook of the Mammals of the World* (Lynx Edicions: Conservation International: IUCN, 2019).

57. S. R. Foss, in *The Evolution of Artiodactyls*, D. R. Prothero, S. E. Foss, Eds. (Johns Hopkins University Press, Baltimore, 2007).

58. P. Myers, R. Espinosa, C. S. Parr, T. Jones, G. S. Hammond, T. A. Dewey, *The Animal Diversity Web (online)* (2021; https://animaldiversity.org).

59. *The Paleobiology Database* (2021; www.paleobiodb.org).

60. C. De Muizon, G. Billet, C. Argot, S. Ladevèze, F. Goussard, Alcidedorbignya inopinata, a basal pantodont (Placentalia, Mammalia) from the early Palaeocene of Bolivia: anatomy, phylogeny and palaeobiology. *Geodiv.* **37**, 397 (2015).

61. J. R. Wible, G. W. Rougier, M. J. Novacek, R. J. Asher, Cretaceous eutherians and Laurasian origin for placental mammals near the K/T boundary. *Nature*. **447**, 1003–1006 (2007).

62. F. Delsuc *et al*., The phylogenetic affinities of the extinct glyptodonts. *Curr. Biol.* **26**, R155–R156 (2016).

63. F. Delsuc *et al.*, Ancient mitogenomes reveal the evolutionary history and biogeography of sloths. *Curr. Biol.* **29**, 2031-2042 (2019).

64. A. E. Zurita, M. L. Taglioretti, L. M. de Los Reyes, F. Cuadrelli, D. G. Poire, Regarding the real diversity of Glyptodontidae (Mammalia, Xenarthra) in the late Pliocene (Chapadmalalan Age/Stage) of Argentina. *Anais da Acad. Bras. de Cienc.* **88**, 809–827 (2016).

65. M. S. Springer *et al*., Interordinal gene capture, the phylogenetic position of Steller's sea cow based on molecular and morphological data, and the macroevolutionary history of Sirenia. *Molec. Phyl. Evol.* **91**, 178–193 (2015).

66. G. Billet, Phylogeny of the Notoungulata (Mammalia) based on cranial and dental characters. *J. Syst. Palaeont.* **9**, 481–497 (2011).

67. F. Welker *et al.*, Ancient proteins resolve the evolutionary history of Darwin's South American ungulates. *Nature*. **522**, 81–84 (2015).

68. J. A. O'Sullivan, "Evolution of the Proximal Third Phalanx in Oligocene-Miocene Equids, and the Utility of Phalangeal Indices in Phylogeny Reconstruction" in *Mammalian Evolutionary Morphology: A Tribute to Frederick S. Szalay*, E. J. Sargis, M. Dagosto, Eds. (Vertebrate Paleobiology and Paleoanthropology Series, Springer Netherlands, Dordrecht, 2008;), pp. 159–165.

69. J. L. A. Paijmans *et al.*, Evolutionary history of saber-toothed cats based on ancient mitogenomics. *Curr. Biol.* **27**, 3330-3336 (2017).

70. A. Berta, M. Churchill, R. W. Boessenecker, The origin and evolutionary biology of pinnipeds: seals, sea lions, and walruses. *Ann. Rev. Earth Planet. Sci*. **46**, 203–228 (2018).

71. R. Weppe, C. Blondel, M. Vianey-Liaud, T. Pélissié, M. J. Orliac, A new Cainotherioidea (Mammalia, Artiodactyla) from Palembert (Quercy, SW France): Phylogenetic relationships and evolutionary history of the dental pattern of Cainotheriidae. *Palaeontol. Electron*. **23**, 1–20 (2020).

72. M. Spaulding, M. A. O'Leary, J. Gatesy, Relationships of Cetacea (Artiodactyla) Among Mammals: Increased Taxon Sampling Alters Interpretations of Key Fossils and Character Evolution. *PLOS ONE*. **4**, e7062 (2009).

73. M. Spaulding, J. J. Flynn, Phylogeny of the Carnivoramorpha: The impact of postcranial characters. *J. Syst. Palaeont*. **10**, 653–677 (2012).

74. R. S. Feranec, Ecological generalization during adaptive radiation: evidence from Neogene mammals. *Evol. Ecol. Res*. **9**, 555–577 (2007).

75. M. Churchill, J. H. Geisler, B. L. Beatty, A. Goswami, Evolution of cranial telescoping in echolocating whales (Cetacea: Odontoceti). *Evol.* **72**, 1092–1108 (2018).

76. G. T. Lloyd, G. J. Slater, A total-group phylogenetic metatree for Cetacea and the importance of fossil data in diversification analyses. *Syst. Biol.* **70**, 922–939 (2021).

77. J. H. Geisler, M. W. Colbert, J. L. Carew, A new fossil species supports an early origin for toothed whale echolocation. *Nature*. **508**, 383–386 (2014).

78. F. G. Marx, R. E. Fordyce, Baleen boom and bust: a synthesis of mysticete phylogeny, diversity and disparity. *Roy. Soc. Open Sci.* **2**, 140434.

79. G. M. Gasparini, M. Ubilla, Platygonus sp. (Mammalia: Tayassuidae) in Uruguay (Raigón? Formation; Pliocene–early Pleistocene), comments about its distribution and palaeoenvironmental significance in South America. *J. Nat. Hist.* **45**, 2855–2870 (2011).

80. N. Rybczynski, M. R. Dawson, R. H. Tedford, A semi-aquatic Arctic mammalian carnivore from the Miocene epoch and origin of Pinnipedia. *Nature*. **458**, 1021–1024 (2009).

81. L. T. Holbrook, J. Lapergola, A new genus of perissodactyl (Mammalia) from the Bridgerian of Wyoming, with comments on basal perissodactyl phylogeny. *J. Vert. Paleont.* **31**, 895–901 (2011).

82. M. C. Mihlbachler, Species taxonomy, phylogeny and biogeography of the Brontotheriidae (Mammalia, Perissodactyla), *Bull. Amer. Mus. Nat. Hist.* **311**, 1-473 (2008).

83. J. Tissier *et al*., New data on Amynodontidae (Mammalia, Perissodactyla) from Eastern Europe: Phylogenetic and palaeobiogeographic implications around the Eocene-Oligocene transition. *PLOS ONE*. **13**, e0193774 (2018).

84. D. Prothero, *The Evolution of North American Rhinoceroses* (Cambridge University Press, 2005)

85. P.-O. Antoine *et al*., A revision of Aceratherium blanfordi Lydekker, 1884 (Mammalia: Rhinocerotidae) from the Early Miocene of Pakistan: postcranials as a key. *Zool. J. Linn. Soc.* **160**, 139–194 (2010).

86. B. A. Williams, R. F. Kay, E. C. Kirk, New perspectives on anthropoid origins. *Proc. Natl. Acad. Sci. U.S.A.*. **107**, 4797–4804 (2010).

87. A. Harrington, M. Silcox, G. Yapuncich, D. Boyer, J. Bloch, First virtual endocasts of adapiform primates. *J. Human Evol.* **99**, 52–78 (2016).

88. J. I. Bloch, M. T. Silcox, D. M. Boyer, E. J. Sargis, New Paleocene skeletons and the relationship of plesiadapiforms to crown-clade primates. *Proc. Natl. Acad. Sci. U.S.A.* **104**, 1159–1164 (2007).

89. S. Hopkins, Phylogeny and evolutionary history of the Aplodontoidea (Mammalia: Rodentia). *Zool. J. Linn. Soc.* **153**, 769–838 (2008).

90. J. J. M. Calede, J. X. Samuels, A new species of Ceratogaulus from Nebraska and the evolution of nasal horns in Mylagaulidae (Mammalia, Rodentia, Aplodontioidea). *J. Syst. Palaeont*. **18**, 1395–1414 (2020).

91. P. Virtanen *et al.*, SciPy 1.0: fundamental algorithms for scientific computing in Python. *Nat. Methods*. **17**, 261–272 (2020).

92. E. W. Goolsby, J. Bruggeman, C. Ané, Rphylopars: fast multivariate phylogenetic comparative methods for missing data and within-species variation. *Meth. Ecol. Evol.* **8**, 22–27 (2017).

93. J. Clavel, G. Escarguel, G. Merceron, mvmorph: an r package for fitting multivariate evolutionary models to morphometric data. *Meth. Ecol. Evol.* **6**, 1311–1319 (2015).

94. J. Clavel, H. Morlon, Reliable Phylogenetic Regressions for Multivariate Comparative Data: Illustration with the MANOVA and Application to the Effect of Diet on Mandible Morphology in Phyllostomid Bats. *Syst. Biol.* **69**, 927–943 (2020).

95. L. J. Revell, Phylogenetic signal and linear regression on species data. *Meth. Ecol. Evol.* **1**, 319–329 (2010).

96. E. A. Housworth, E. P. Martins, M. Lynch, The phylogenetic mixed model. *Am. Nat*. **163**, 84–96 (2004).

97. R. P. Freckleton, P. H. Harvey, M. Pagel, Phylogenetic analysis and comparative data: a test and review of evidence. *Am. Nat*. **160**, 712–726 (2002).

Acknowledgments: We are indebted to the numerous colleagues, curators, and collections staff at international museums that provided access to specimens for this project, in particular Roberto Portela Miguez, Roula Pappa, Pip Brewer, Richard Sabin, and Louise Tomsett (NHM), Pierre-Henri Fabre (Université de Montpellier), Judy Galkin, Ruth O'Leary, and Alana Gishlick (AMNH), Gertrud Rößner (BSP), S. and R. Boessenecker (CCNHM), Bill Simpson (FMNH), Desui Miao (KU), Judith Chupasko (MCZ), Sam McLeod,

Xiaoming Wang, and Jorge Velez-Juarbe (LACM), Jack Ashby and Paolo Viscardi (LDUCZ), Marcelo Reguero (MLP), Guillaume Billet, Jacques Cuisin, and Geraldine Veron (MNHN), Pat Holroyd, Mark Goodwin, and Jack Tseng (UCMP), Bill Sanders (UMMP), Amanda Millhouse and Suzanne Peurach (USNM), Chris Norris and Dan Brinkman (YPM), Ross Secord and George Carter (UNSM), and Loic Costeur (NMB). We are grateful to Vincent Fernandez and Brett Clark (NHM) and Jonathan Keller (UMN) for support in microCT scanning and to the 'plate-forme de morphometrie' of the UMS 2700 (CNRS, MNHN) for access to the surface scanner. We thank Emily Watt (NHM/UCL) for uploading scans to online repositories. We are grateful to the two anonymous reviewers and the editor for their thoughtful comments. We thank V. Herridge for putting a name to this phenomenon.

Funding: European Research Council grant STG-2014-637171 (AG)

National Science Foundation SF-EAR 1349607 (JG, BB, AG, MC)

Gerstner Scholar Postdoctoral Research Fellowship (AC, NS)

Natural Environment Research Council Doctoral Training Partnership training grant NE/L002485/1 (EC)

Horizon 2020 MCSA Fellowship IF 797373-EVOTOOLS (JC)

National Science Foundation EAR 1338262 (DLF)

Labex BCDiv 10-LABX-0003 (ACF)

Author contributions:

Conceptualization: AG

Methodology: AG, RNF, JC, ACF, AW

Software: AG, RNF, JC, AW, ACF

Investigation: AG, RNF, EN, JC, EC, ACF, TJDH, AC, MC, BB, JG, NS, DLF

Visualization: AG, RNF

Funding acquisition: AG, EC, JG, BB, AC, NS

Writing – original draft: AG

Writing – review & editing: AG, RNF, EN, JC, EC, ACF, TJDH, AC, MC, BB, JG, NS, DLF, AW

Competing interests: Authors declare that they have no competing interests.

Data and materials availability: Morphometric data and novel code are provided on Github (https://github.com/anjgoswami/Goswami_et_al_Placental_evolution_2022). 3D meshes for all specimens are available for free download on Phenome10k.org or Morphosource.org, as detailed in data S1, unless specifically restricted by specimen repositories. All specimen and species details, including physical and online repository information and trait data, are provided in data S1.

Supplementary Materials:

Supplementary Materials and Methods

Figures S1 to S8

Tables S1 to S2

Data S1

References (*23–97*)

Figure captions

Figure 1. Cranial variation across placental mammals is highly concentrated. A) Cranial morphospace for placental mammals showing PC1-3, with density contours reflecting three concentrations of placental mammal skull shapes, two dominated by single clades, and highlighting specimens along the edges of each of the high-density regions. B) Detailed morphospace of PC1-2, showing superordinal and ordinal affiliations of specimens and wireframe models of the variation along each axis. Symbols and colours in the morphospace indicate clade affiliation, as described on the legend (version with color-blind palette provided in figure S2). Colours on skull wireframes denote different cranial elements (see table S1 for details).

Figure 2. Rapid evolutionary rates are observed near the base of several placental mammal clades. Estimated branch-specific rates of cranial evolution using a variable-rates Brownian motion model with a lambda tree transformation, shown here for one example tree (Topology 2, root age 80-85Ma, tree 85 of 100). Warmer and cooler colors indicate faster and slower rates of evolution, respectively, with yellow indicating moderate rates. Fast branches are concentrated within Cetacea, indicated with a whale icon, as well as more basal branches for several orders. A subset of the sampled skulls is positioned proximal to their terminal branches to demonstrate the immense cranial diversity of living and extinct placentals. Geological age is indicated by alternating shading of circles, from innermost outwards: Cretaceous, Paleogene, Neogene, Quaternary.

Figure 3. Rates of evolution peak early in placental mammal evolution and attenuate through time. A) Rates of evolution through time are shown for one sample tree per root age for

topology 2, colored by root age, while clade-specific tip rates and ancestral estimates are shown for topology 2, root age 80-85, tree 85, as in Fig. 2. The Cretaceous-Paleogene (K/Pg) boundary and the Paleocene-Eocene Thermal Maximum (PETM) are indicated with red and green lines, respectively. B) Subsetting terminal branch rates by each order demonstrates the slow pace of evolution in stem placental mammals and euarchontoglirans, in contrast to Afrotheria and several laurasiatherian clades. * indicates wholly extinct orders. Estimated ancestral cranial shapes (excluding teeth and bullae) for C) Placentalia and D) each superorder, using *Vulpes pallida* for the reference mesh, suggest remarkable similarity among the estimated MRCAs for placental mammal superorders.

Figure 4. Aquatic, herbivorous, precocial, and social placental mammals evolve at the fastest rates. Rates of evolution based on ecological and life history traits for placentals, with diet and locomotion estimated for all living and extinct taxa sampled, while the other four categories are limited to extant taxa. Distributions represent results from 100 sampled trees for topology 2, root age 80-85.

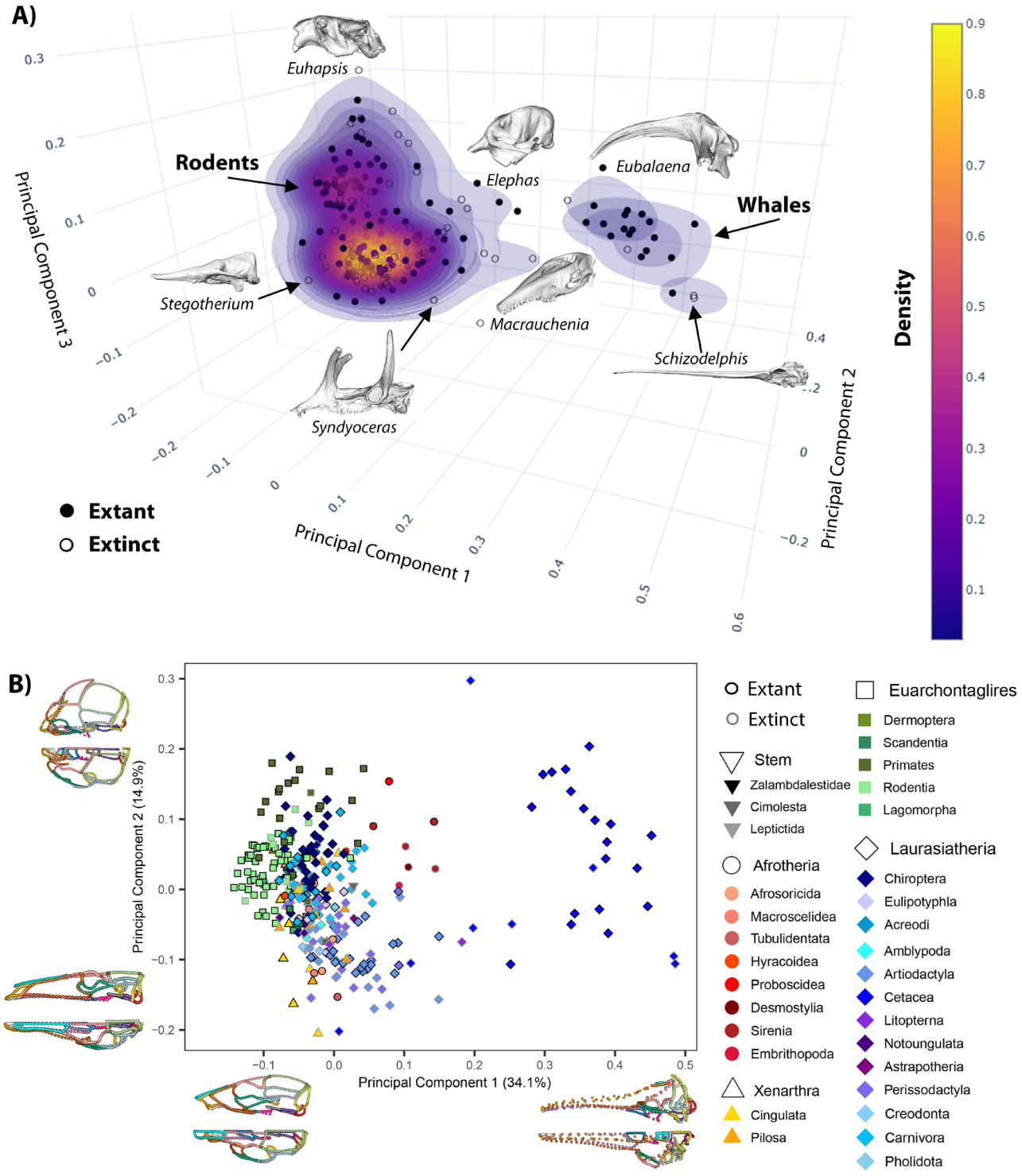

Figure 1. Cranial variation across placental mammals is highly concentrated.

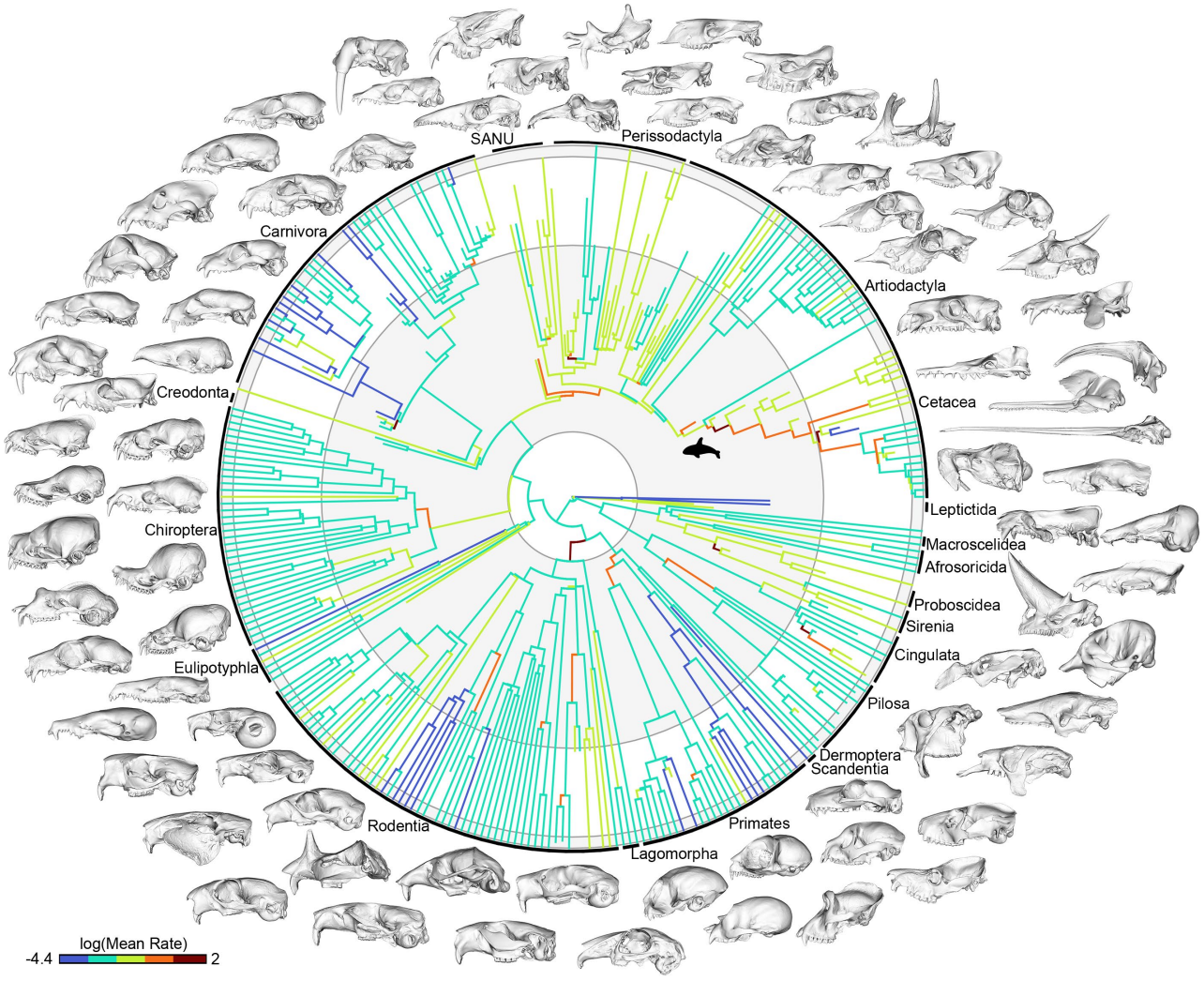

Figure 2. Rapid evolutionary rates are observed near the base of several placental mammal clades.

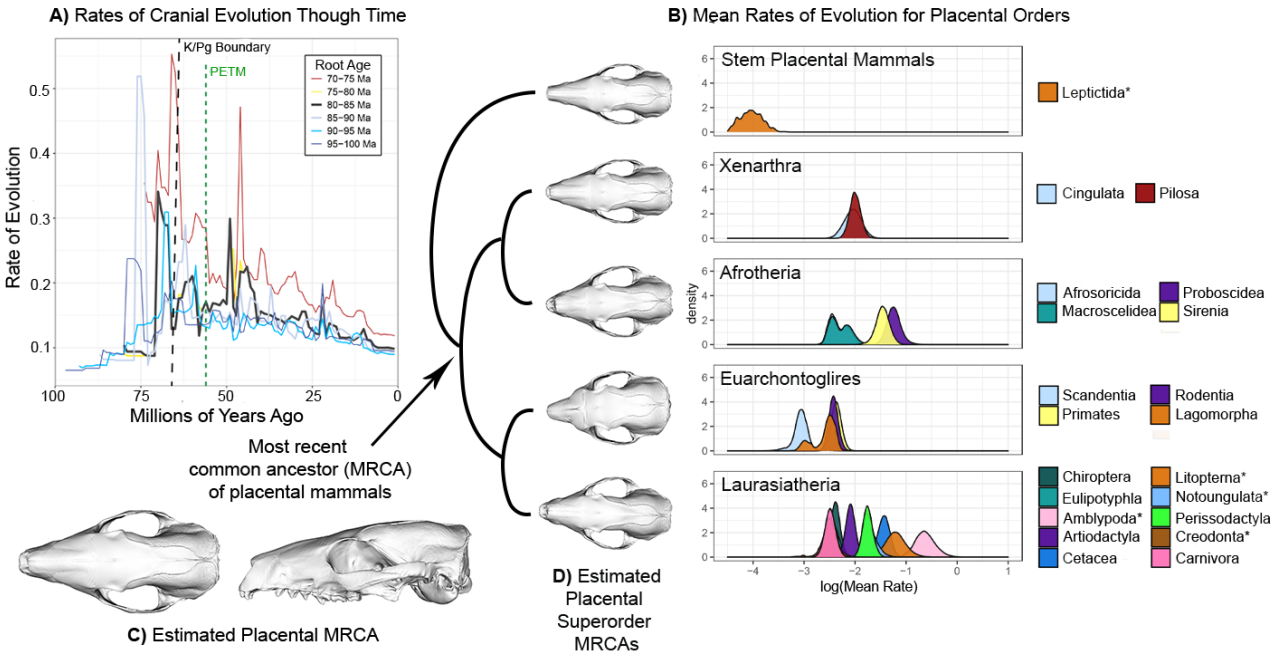

Figure 3. Rates of evolution peak early in placental mammal evolution and attenuate through time.

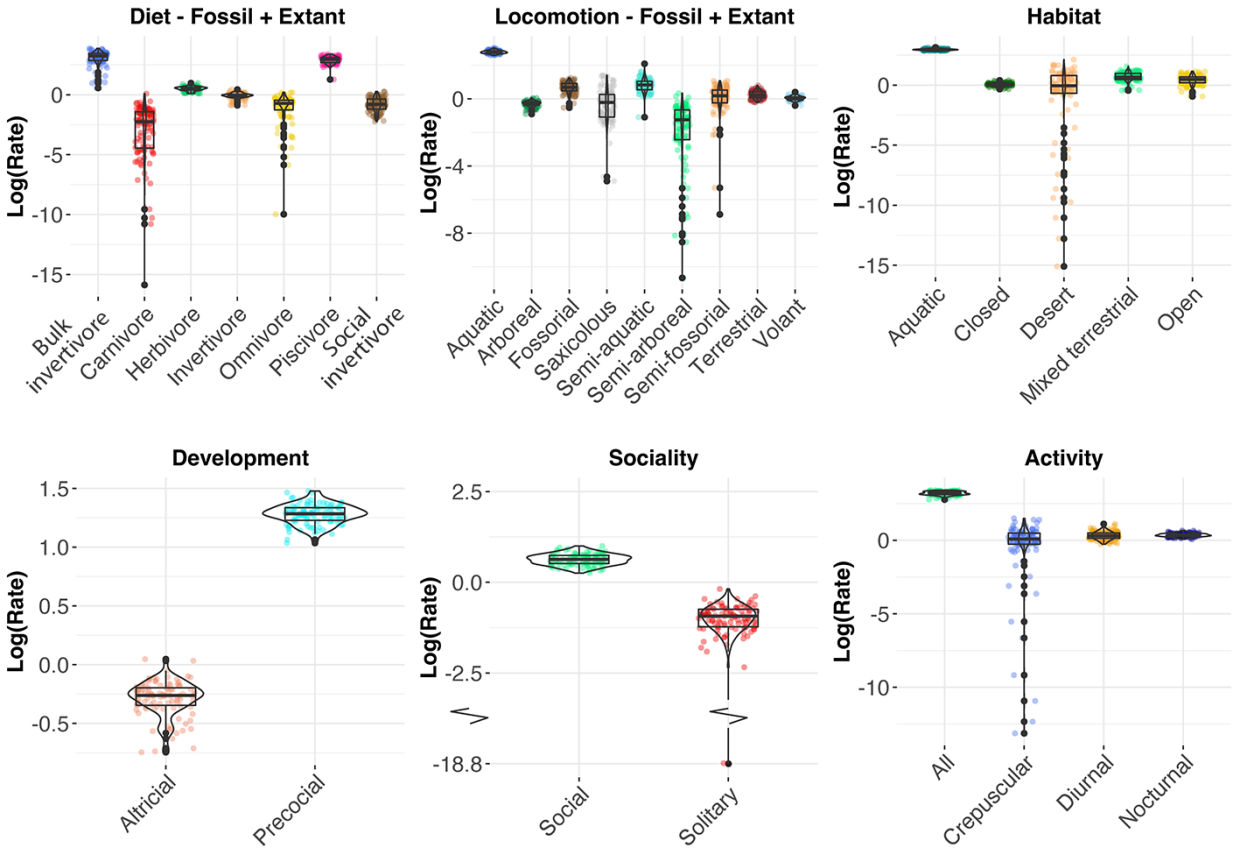

Figure 4. Aquatic, herbivorous, precocial, and social placental mammals evolve at the fastest rates.